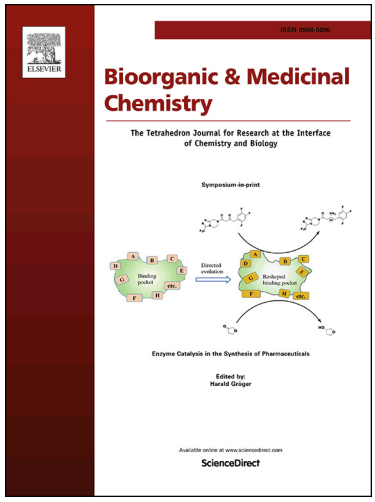

Discovery of Novel Syk/PDGFR-α/c-Kit Inhibitors as Multi-targeting Drugs to Treat Rheumatoid Arthritis

Xiaokang Li, Yahui Huang, Junfei Chen, Lingling Zhang, Fei Mao, Jin Zhu, Chunquan Sheng, Jian Li

PII: S0968-0896(18)30668-0
DOI: https://doi.org/10.1016/j.bmc.2018.06.029
Reference: BMC 14421

To appear in: *Bioorganic & Medicinal Chemistry*

Received Date: 3 April 2018
Revised Date: 14 June 2018
Accepted Date: 21 June 2018

Please cite this article as: Li, X., Huang, Y., Chen, J., Zhang, L., Mao, F., Zhu, J., Sheng, C., Li, J., Discovery of Novel Syk/PDGFR-α/c-Kit Inhibitors as Multi-targeting Drugs to Treat Rheumatoid Arthritis, *Bioorganic & Medicinal Chemistry* (2018), doi: https://doi.org/10.1016/j.bmc.2018.06.029

Discovery of Novel Syk/PDGFR-α/c-Kit Inhibitors as Multi-targeting Drugs to Treat Rheumatoid Arthritis

Xiaokang Li,[1, †] Yahui Huang,[2, †] Junfei Chen, [2, †] Lingling Zhang,[1] Fei Mao,[1] Jin Zhu,[1] Chunquan Sheng,[2,*] Jian Li[1,*]

[1] *Shanghai Key Laboratory of New Drug Design, School of Pharmacy, East China University of Science & Technology, 130 Meilong Road, Shanghai 200237, People's Republic of China*

[2] *Department of Medicinal Chemistry, School of Pharmacy, Second Military Medical University, 325 Guohe Road, Shanghai 200433, People's Republic of China*

[#]These three authors contributed equally to this work.

* To whom correspondence should be addressed.

For C. Sheng: Phone/Fax, 86-21-81871205, E-mail, shengcq@smmu.edu.cn;

For J. Li: Phone/Fax 86-21-64252584, E-mail, jianli@ecust.edu.cn

Abstract

Due to the complex biological pathways involved in rheumatoid arthritis, discovery of multi-targeting small molecules provides an effective strategy to achieve better efficacy and lower toxicity. Herein the first Syk/PDGFR-α/c-Kit inhibitors were designed and evaluated. Dihydrofuropyrimidine derivative **13** showed potent inhibitory activity against the three targets. Importantly, compound **13** exhibited good cellular efficacy against fibroblast-like synoviocytes (IC_{50} = 3.21 μM) and mouse bone marrow-derived mast cells (IC_{50} = 2.03 μM) and significantly decreased the secretion of inflammatory cytokines. Thus, Syk/PDGFR-α/c-Kit triple inhibitor **13** represented a promising lead compound for the treatment of RA.

Keywords: Rheumatoid arthritis; Syk; PDGFR-α; c-Kit; multi-targeting inhibitors; dihydrofuropyrimidines

1. Introduction

Rheumatoid arthritis (RA) is a chronic and multi-factorial autoimmune disorder, affecting approximately 0.5-1% of the adult population.[1] RA is characterized by the accumulation and proliferation of inflammatory cells in the synovial lining, resulting in the formation of pannus tissue and the erosion of cartilage and bone. In RA patients, mast cells and fibroblast-like synoviocytes (FLSs) are activated and contribute to synovial inflammation and joint destruction. The relationship of FLS and mast cells with joint damage and the propagation of inflammation has been well established.[2] Fibroblasts express platelet-derived growth factor receptor (PDGFR) and proliferate in response to a variety of PDGF ligands. Both PDGFR and its ligands are overexpressed in RA synovial tissue, and PDGF is a potent stimulant of synovial hyperplasia in RA.[3] In addition, increased number of mast cells were found in the synovium of RA patients.[2] The activation of mast cell resulted in the release of mediators, such as tumor necrosis factor-α (TNF-α), contributing to the inflammatory and destructive processes of RA. Stem cell factor (SCF) is essential for the growth and survival of mast cells, which also functions as the ligand of c-Kit receptor.[4] Thus, the inhibition of c-Kit signaling might prevent mast cell activity in the synovium of RA patients. Imatinib[5] and masitinib (**1**)[6] are multi-targeted kinase inhibitors (**Fig. 1**) with potent inhibitory activities against c-Kit and PDGFR, which also showed considerable antirheumatic efficacy. Masitinib is currently evaluated as a RA therapeutic drug in phase II/III clinical trials.[7]

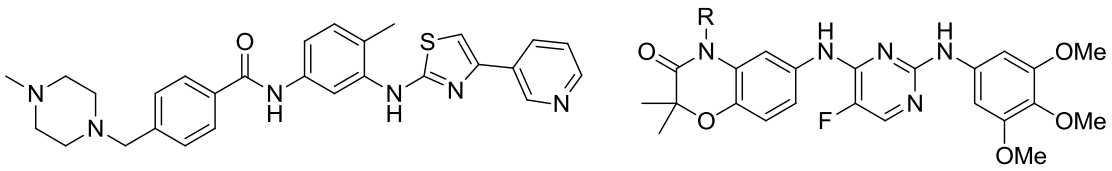

1 (mastinib)

2 R = H
3 R = $CH_2OP(O)(ONa)_2$

Fig. 1. Chemical structures of the masitinib (**1**), R406 (**2**) and fostamatinib disodium (**3**).

Spleen tyrosine kinase (Syk) represents a promising target for the treatment of RA.[8] As an intracellular cytoplasmic non-receptor tyrosine kinase, Syk plays an important role in the production of cytokine and metalloproteinase in RA FLSs. A number of Syk inhibitors were developed and several of them, such as R406 (**2**)[9] and fostamatinib disodium (**3**)[10], have been evaluated in clinical trials (**Fig. 1**).[11] However, clinical development of Syk inhibitors was mainly hampered by adverse effects including diarrhea, upper respiratory tract infection, neutropenia, hypertension and so on.[12] To overcome the drawbacks of the unsuccessful clinical candidates, discovery of new Syk inhibitors with improved efficiency and selectivity is still an active area.[13] Alternatively, Syk-based multi-targeting inhibitors offer a new opportunity for the treatment of RA.

Autoimmune disorders are regulated by complex biological pathways. Rather than inhibiting a single target, blocking multi-targets would be advantageous to achieve better efficacy and lower toxicity. Herein, the first Syk/PDGFR-α/c-Kit inhibitors were discovered, which showed potent anti-inflammatory activity. The proof-of-concept study provided a new strategy for the treatment of RA.

2. Chemistry

The general procedure for the synthesis of thiazolopyrimidine diamine derivatives was outlined in **Scheme 1**. Starting from commercially available **4**, intermediate **5** was prepared through a nucleophilic aromatic substitution reaction with various primary amines (R-NH_2). In the presence of DIPEA and NMP, compound **5** reacted with *tert*-butyl pyrrolidin-3-ylcarbamate under the microwave condition to afford intermediate **6**. Then, it was transformed into intermedate **9** by the condensation reaction with mono-benzylbenzoate **8**, which was synthesized by the subsituion reaction between acid **7** and benzyl bromide. Finally, target compounds **10**-**23** were prepared by deprotection of the

benzyl group in the presence of Pd/C and methanol.

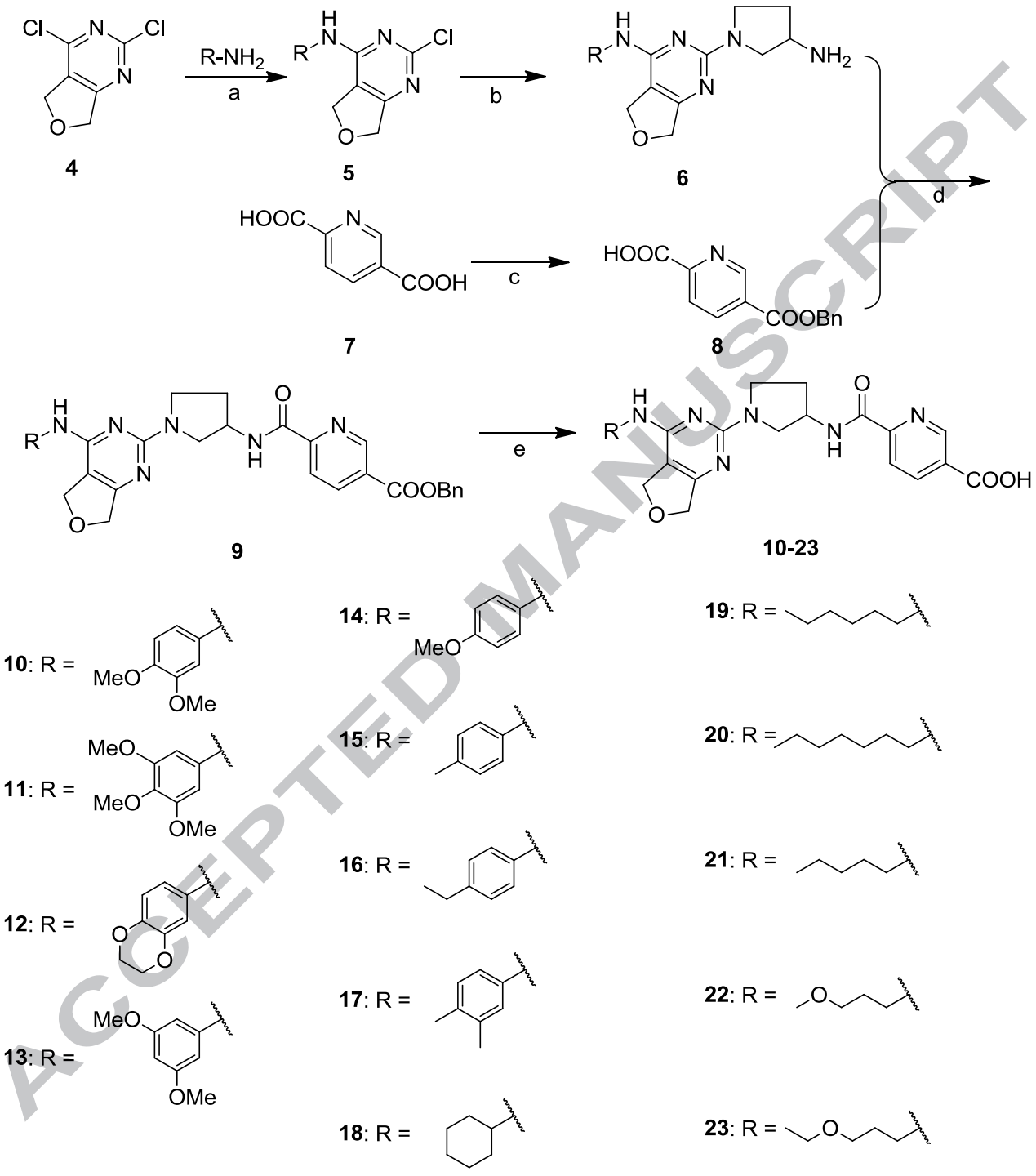

Scheme 1. Synthesis of dihydrofuropyrimidine diamine derivatives **10-23**. *Reagents and conditions:* (a) DIPEA, DMSO, 60 ^{o}C, overnight, 65%; (b) *tert*-butyl pyrrolidin-3-ylcarbamate, DIPEA, NMP, M.W., 80 W, 140 ^{o}C, 1 h, 49%; (c) (i) Triethylamine, methanol, overnight, r.t., (ii) Benzyl bromide, DMF, 100 ^{o}C, 2 h, 17% over two steps; (d) HATU, DIPEA, DMAP, EDCI, DMF, 24 h, 63%; (e)

Pd/C, methanol, overnight, 34%

3. Results and discussion

3.1 Design of Syk/PDGFR-α/c-Kit Inhibitors

Thiazolopyrimidine diamines were selective Syk inhibitors developed by Roche.[13] However, poor physicochemical properties hampered them from further development. Herein the thiazolopyrimidine diamine scaffold was used as the starting point for drug design (**Fig. 2**). The thiazolopyrimidine core was replaced by dihydrofuropyrimidine to form favorable interactions with Syk/PDGFR-α/c-Kit (for detail see **Fig. 5**). Also, the dihydrofuropyrimidine scaffold and the benzene/pyridine replacement were favorable for improving the water solubility (**Table S2** in **supporting information**). As a result, dihydrofuropyrimiddine derivatives **10**-**23** were designed and synthesized. Besides, two cyclopentapyrimidine diamine derivatives (**29** and **31**) were designed and synthesized to investigate the importance of the scaffold oxygen atom and the terminal COOH (**Scheme S1** in **supporting information**).

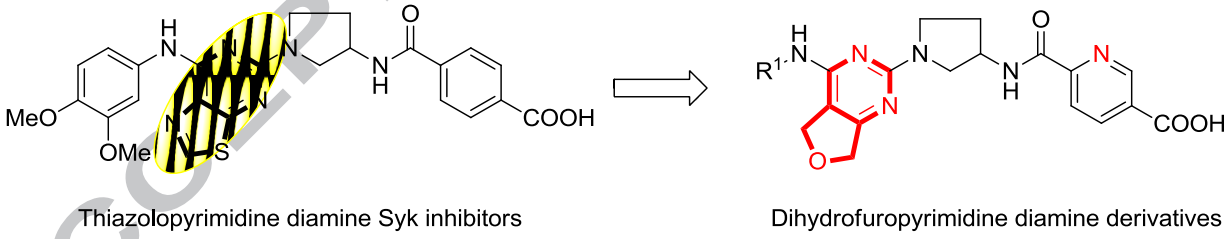

Fig. 2. The design rationale of dihydrofuropyrimidine diamine Syk/PDGFR-α/c-Kit inhibitors.

3.2 Syk/PDGFR-α/c-Kit Inhibitory Activities and Structure-Activity Relationships

Syk, PDGFR-α and c-Kit inhibitory activities of the target compounds were assayed (**Table 1**). Compound **10** showed moderate inhibitory activity against Syk (IC_{50} = 23.7 μM) and PDGFR-α (IC_{50} = 28.1 μM). However, it was inactive against c-Kit. Interestingly, after the introduction of an

additional methoxyl group at position 5, trimethoxyl derivative **11** was proven to be a Syk (IC_{50} = 14.2 μM), PDGFR-α (IC_{50} = 2.2 μM) and c-Kit (IC_{50} = 31.3 μM) triple inhibitor. Then, a series of derivatives (**12-23**) were designed and synthesized by varying the amine substitutions. Syk/PDGFR-α/c-Kit inhibitory activity was retained for 3,5-dimethoxyl derivative **13**. When the 3,4-methoxyl group was fused into 1,4-dioxane, compound **12** was a Syk/c-Kit dual inhibitor, whose PDGFR-α inhibitory activity was lost. Removal of 3-methoxyl group of compound **10** led to the loss of PDGFR-α and c-Kit inhibitory activity (compound **14**). Similarly, 4-ethyl (**16**) and 3,4-dimethyl (**17**) derivatives were only effective against Syk. When the phenyl group of compound **10** was replaced by various alkyl groups, compounds **18-23** were inactive against PDGFR-α and c-Kit. Among them, compounds **21-23** lost the activity against all the three targets. In addition, removing the oxygen atom of the scaffold (compound **31)** resulted in less potent Syk inhibitory activity (IC_{50} = 25.3 μM) than compound **10** (IC_{50} = 23.7 μM). Moreover, after the esterification of carboxyl group, compound **29** was totally inactive against Syk (IC_{50} > 50 μM), indicating that the importance of the carboxyl group for the Syk inhibitory activity (**Table S1** in supporting information).

Table 1 Chemical structures and anti-Syk assay results of compounds **10**-**23**.

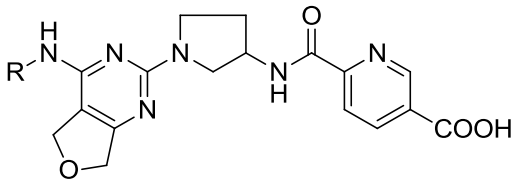

Compounds	R	Syk IC_{50} (μM)	PDGFR-α IC_{50} (μM)	c-Kit IC_{50} (μM)
10	3,4-dimethoxyphenyl	23.7	28.1	> 50

11	3,4,5-trimethoxyphenyl	14.2	2.2	31.3
12	2,3-dihydrobenzo[*b*][1,4]dioxin-6-yl	20.3	> 50	49.2
13	3,5-dimethoxyphenyl	20.9	7.5	18.6
14	4-methoxyphenyl	32.1	> 50	> 50
15	4-methylphenyl	20.9	> 50	> 50
16	4-ethylphenyl	19.2	> 50	> 50
17	3,4-dimethylphenyl	15.6	> 50	> 50
18	cyclohexyl	13.5	> 50	> 50
19	hexyl	9.7	> 50	> 50
20	heptyl	11.4	> 50	25.8
21	pentyl	> 50	> 50	> 50
22	3-methoxypropyl	> 50	> 50	> 50
23	3-ethoxypropyl	> 50	> 50	> 50

3.3 Cellular Potency of the Selected Compounds

According to the Syk, PDGFR-α and c-kit inhibitory activity, seven compounds (**11**, **13**, **16-20)** were selected to evaluate their potency on FLSs-RA proliferation, using compound **2** as the reference drug. As shown in **Table 2**, most compounds were capable of inhibiting FLSs proliferation and five of them (**13**, **16**, **18-20**) showed potent cellular inhibitory activity with IC_{50} value lower than 10 μM. On the basis of the cellular potency, two compounds (**13** and **19**) were selected to evaluate whether the addition of inhibitors could block the production of inflammatory cytokines, such as interleukin-6 (IL-6) and metalloproteinase-3 (MMP-3). The results indicated that both compounds decreased the production of IL-6 and MMP-3 in a concentration-dependent manner (**Fig. 3**). In particular, compound **13** exhibited comparable potency to positive control **2** at

the concentration of 15 μM.

Table 2 Effects of preferred compounds on FLSs-RA proliferation.

Compounds	**2**	**11**	**13**	**16**	**17**	**18**	**19**	**20**
IC_{50} (μM)	14.6	31.0	3.2	9.4	11.2	5.4	4.0	8.1

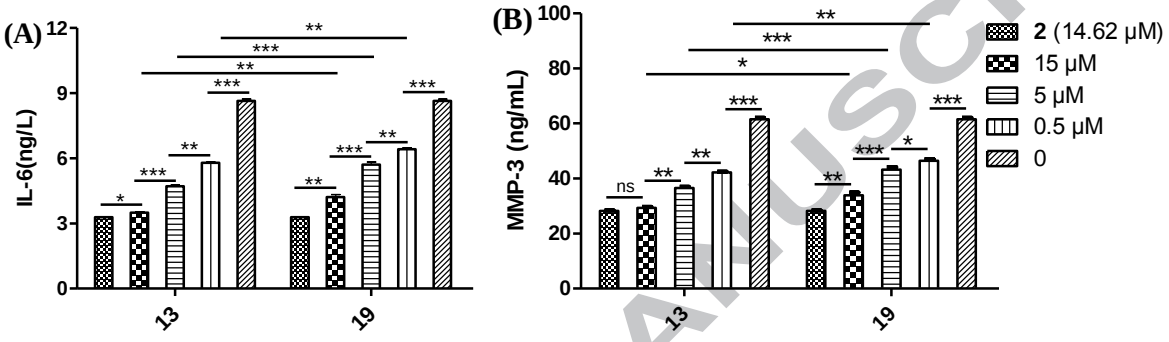

Fig. 3. Effects of compounds **13** and **19** on inflammatory cytokine production of IL-6 (**A**) and MMP-3 (**B**) from FLSs.

Three compounds (**11**, **13** and **20**) were subjected to the mast cell assay using masitinib as the positive control. Masitinib exhibited strong potency to inhibit the proliferation of mouse bone marrow-derived mast cells (mBMMCs). However, all of our three compounds were less effective (**Table 3**), possibly due to moderate inhibitory activity against the three kinases. The most promising compound **13** exhibited the inhibitory activity with an IC_{50} value of 2 μM. Compounds **13** and **20** were further evaluated the ability to decrease the release of TNF-α. Two compounds both concentration-dependently decreased the release of TNF-α, and compound **13** showed better potency (**Fig. 4**).

Table 3 Effects of compounds **11**, **13** and **20** on mBMMCs proliferation.

Compounds	**1**	**11**	**13**	**20**
IC_{50} (μM)	0.1	21.1	2.0	13.0

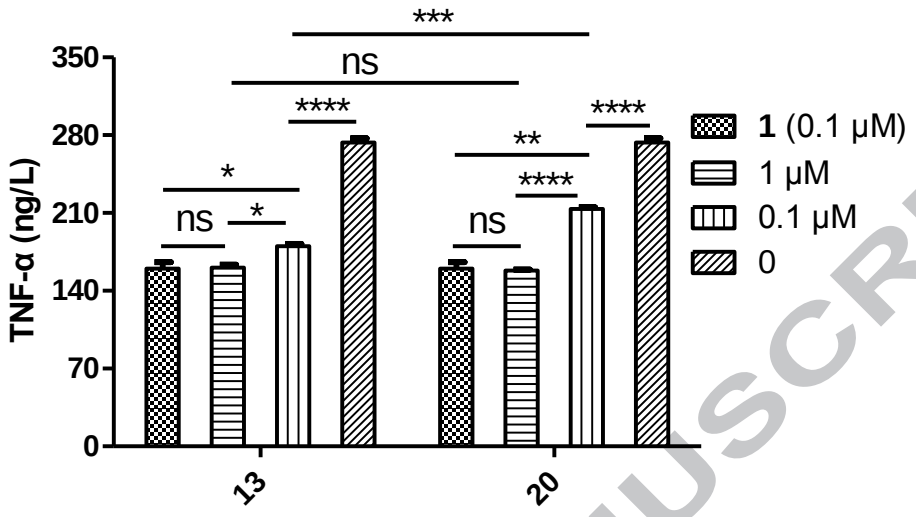

Fig. 4. Effects of compounds **13** and **20** on TNF-α production from mBMMCs.

*3.4 Binding Mode of Compound **13** with Syk/PDGFR-α/c-Kit*

In order to investigate the binding modes of compound **13** with Syk, PDGFR-α and c-Kit, molecular docking studies were performed. As shown in **Fig. 5A**, the dihydrofuropyrimidine diamine scaffold of compound **13** formed a hydrogen bond to the backbone of Ala451 in the hinge region of Syk (PDB ID: 1XBC[14]). Moreover, its carboxyl group formed additional hydrogen bonding interaction with Lys533. For c-Kit (PDB ID: 1T46[15]), the carbamoylnicotinic acid group formed two hydrogen bonds with Glu640 and Thr670 in the hinge region of c-Kit (**Fig. 5B**). Furthermore, an additional hydrogen bond was observed between the 5-methoxyl group and Ile571, which might be the reason why **13** was more potent than 3,4-dimethyoxyl derivative **10** against c-Kit. For the binding mode of **13** with PDGFR-α (PDB ID: 5GRN[16]), Asp836 formed two hydrogen bonds with the dihydrofuropyrimidine diamine scaffold and the terminal carboxyl group (**Fig. 5C**). The pyrimidine moiety formed π-π interactions with Lys627.

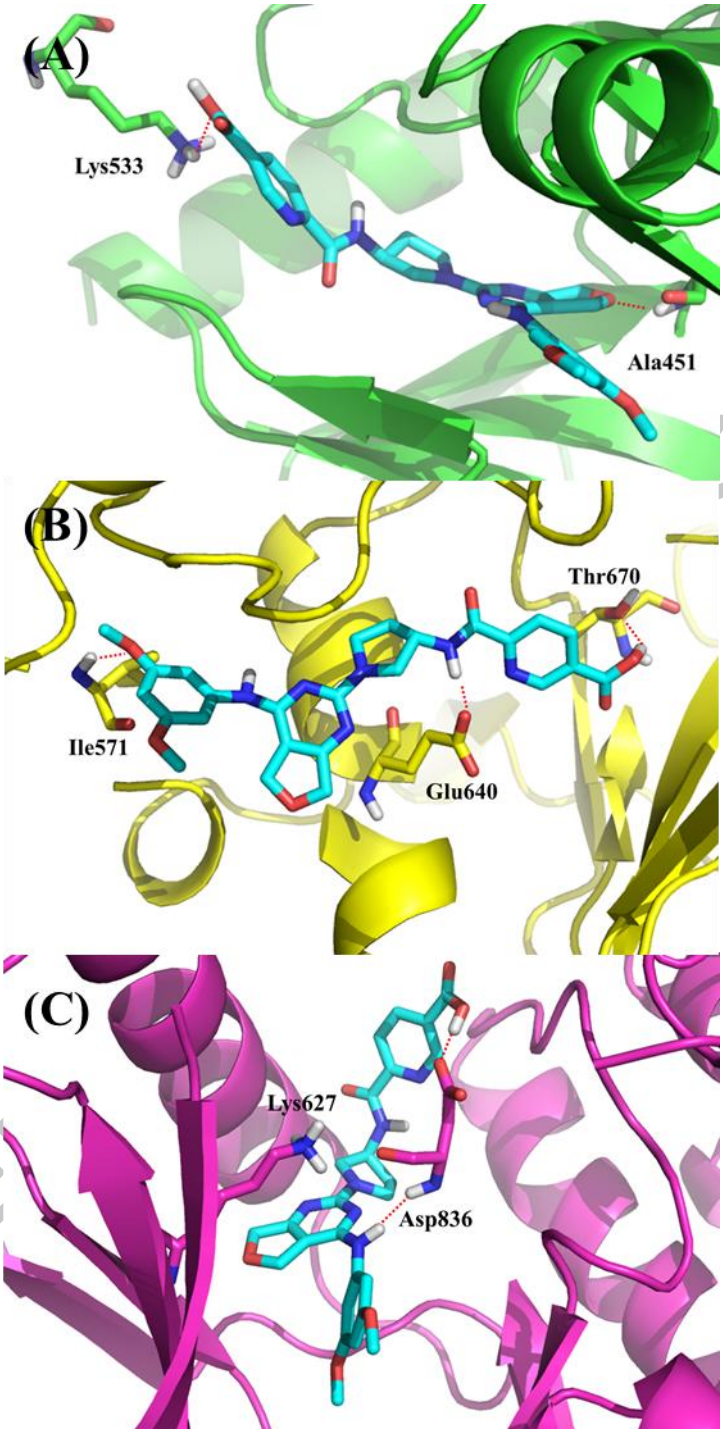

Fig. 5. Proposed binding mode of compound **13** in the active site of Syk (PDB ID: 1XBC, **A**), c-Kit (PDB ID: 1T46, **B**) and PDGFR-α (PDB ID: 5GRN, **C**). Hydrogen bonds are indicated with dashed lines. The figure was generated using PyMol (http://www.pymol.org/).

4. Conclusions

In summary, novel dihydrofuropyrimidine Syk/PDGFR-α/c-Kit triple inhibitors were designed and synthesized. Compound **13** showed relatively balanced inhibitory activity against the three targets. Molecular docking studies revealed that it bound with the three kinases mainly through hydrogen bonding and hydrophobic interactions. Importantly, compound **13** exhibited potent cellular efficacy. It possessed good anti-proliferative activities against FLSs and mBMMCs with IC_{50} values of 3.21 μM and 2.03 μM, respectively, and significantly decreased the secretion of inflammatory cytokine. Thus, compound **13** represented a promising lead compound for further investigation. The discovery of Syk/PDGFR-α/c-Kit inhibitors could serve as a new strategy for the treatment of RA. Further structural optimization will focus on improving the inhibitory activity against Syk/PDGFR-α/c-Kit and adjusting the physicochemical properties.

5. Experimental Section

5.1 Chemistry

Synthetic starting materials, reagents and solvents were purchased from Alfa Aesar, Acros, Adamas-beta, Energy Chemical, J&K, Shanghai Chemical Reagent Co. and TCI at the highest commercial quality and used without further purification. Analytical thin-layer chromatography (TLC) was performed on HSGF 254 (150-200 μm thickness; Yantai Huiyou Co., China), and the components were visualized by observation under UV light (254 nm and 365 nm). Melting points were determined on a SGW X-4 melting point apparatus without correction. The products were purified by recrystallization or column chromatography on silica gel (200-300 mesh). Reaction yields were not optimized. Nuclear magnetic resonance (NMR) spectroscopy was performed on a Bruker AMX-400 NMR spectrometer using deuterated chloroform ($CDCl_3$), deuterated methanol

(CD_3OD), or deuterated dimethyl sulfoxide (DMSO-d_6) as the solvent. Chemical shifts were reported in parts per million (ppm, δ) downfield from tetramethylsilane. Proton coupling patterns were described as singlet (s), doublet (d), triplet (t), quartet (q), multiplet (m), and broad (br). Low- and high-resolution mass spectra (LRMS and HRMS) were given with electron spray ionization (ESI) produced by a Finnigan MAT-95 and a LCQ-DECA spectrometer. HPLC data analysis of compounds **2-31** were performed on an Agilent 1100 with a quaternary pump and diode-array detector (DAD). The peak purity was verified with UV spectra. All analogs were confirmed to be > 95% pure.

*5.1.1 2-Chloro-N-(3,4-dimethoxyphenyl)-5,7-dihydrofuro[3,4-d]pyrimidin-4-amine (**5**).*

A solution of 2,4-dichloro-5,7-dihydrofuro[3,4-*d*]pyrimidine (**4**, 1.89 g, 10 mmol) in DMSO (10 mL) was added commercially available 3,4-dimethoxyaniline (1.53 g, 10 mmol) and DIPEA (2.58 g, 20 mmol). The solution was heated to 60 ºC and stirred overnight. Then the solution was poured into water and extracted with EtOAc, the organic layer was washed by brine, dried with anhydrous Na_2SO_4, and filtered and concentrated under reduced pressure. The crude product was further purified by flash chromatography on silica gel (EtOAc/hexane = 1:1) to afford compound **5** (2.00 g, yield 65%) as an off-white solid. ^{1}H NMR (400 MHz, $CDCl_3$) δ: 6.90-6.81 (m, 3H), 4.88 (s, 2H), 4.42 (s, 2H), 3.92 (s, 3H), 3.89 (s, 3H).

*5.1.2 2-(3-Aminopyrrolidin-1-yl)-N-(3,4-dimethoxyphenyl)-5,7-dihydrofuro[3,4-d]pyrimidin-4-amine (**6**).*

A solution of compound **5** (1.85 g, 6.02 mmol) in 1-methyl-2-pyrrolidinone (2 mL) was added *tert*-butyl pyrrolidin-3-ylcarbamate (1.68 g, 0.90 mmol) and DIPEA (1.55 g, 12.04 mmol). The reaction was conducted under the microwave condition. The solution was heated to 140 ºC under 80 W for 1 h, and then the mixture was concentrated under reduced pressure. The crude product was

purified by flash chromatography on silica gel (MeOH/CH_2Cl_2 = 1: 8) to afford compound **6** (1.05 g, yield 49%) as a brown solid. ^{1}H NMR (400 MHz, DMSO-d_6) δ: 8.53 (s, 1H), 7.41-7.34 (m, 1H), 7.30 (dd, *J* = 8.7, 2.4 Hz, 1H), 6.91 (t, *J* = 7.6 Hz, 1H), 4.24 (q, *J* = 7.0 Hz, 2H), 3.72 (t, *J* = 11.1 Hz, 6H), 2.71 (dd, *J* = 14.2, 7.1 Hz, 4H), 2.08-1.96 (m, 2H), 1.27 (dd, *J* = 9.0, 5.2 Hz, 3H).

*5.1.3 5-((Benzyloxy)carbonyl)picolinic acid (**8**).*

A solution of pyridine-2,5-dicarboxylic acid (**7**, 1.67 g, 10 mmol) in MeOH (50 mL) was added triethylamine (1.52 mL, 11 mmol) dropwisely, and the solution was stirred overnight. The solvent was evaporated under the reduced pressure. The residue was resolved in DMF (10 mL) and added benzyl bromide (1.2 mL) dropwisely. The solution was heated to 100 ºC for 2 h. Then the mixture was poured into water, acidified with diluted HCl and extracted by EtOAc. The organic layer was washed by brine, dried with anhydrous Na_2SO_4, filtered and concentrated under the reduced pressure. The crude product was further purified by flash chromatography on silica gel (EtOAc/hexane = 1: 1) to afford compound **8** (0.44 g, yield 17%) as a white solid. ^{1}H NMR (400 MHz, DMSO-d_6) δ: 9.39 (s, 1H), 8.43 (d, *J* = 7.5 Hz, 1H), 8.12 (d, *J* = 7.4 Hz, 1H), 7.53 (d, *J* = 7.2 Hz, 2H), 7.41 (dt, *J* = 23.2, 7.2 Hz, 3H), 5.41 (s, 2H).

*5.1.4 6-((1-(4-((3,4-Dimethoxyphenyl)amino)-5,7-dihydrofuro[3,4-d]pyrimidin-2-yl)pyrrolidin -3-yl)carbamoyl)nicotinic acid (**10**).*

A solution of compound **6** (0.21 g, 0.58 mmol) in DMF (5 mL) was added intermediate **8** (0.15 g, 0.58 mmol), DIPEA (0.20 mL, 1.16 mmol), HATU (0.21 g, 1.16 mmol). After stirring for 2 h, EDCI (0.22 g, 1.16 mmol) and DMAP (0.14 g, 1.16 mmol) were added into the solution and the resulting mixture was stirred overnight. The solution was poured into water and extracted by EtOAc and the organic layer was washed by brine, dried with anhydrous Na_2SO_4, filtered and concentrated under

reduced pressure to obtain the crude product **9** (0.22 g, yield 63%) without further purification. Then compound **9** was dissolved in MeOH (20 mL) followed by the addition of 10% Pd/C (0.001 mmol). The mixture was stirred under the H_2 atmosphere overnight. The catalyst was filtered off and the combined organic solution was concentrated under reduced pressure to afford target compound **10** (0.046 g, yield 44%) as an off-white solid. ^{1}H NMR (400 MHz, DMSO) δ: 9.15 (s, 1H), 8.94 (s, 1H), 8.59 (s, 1H), 8.42 (s, 1H), 8.09 (s, 1H), 7.62 (s, 1H), 7.21 (s, 1H), 6.89 (s, 1H), 4.89 (s, 2H), 4.68 (s, 2H), 4.51 (s, 1H), 4.37 (s, 1H), 3.71 (s, 6H), 3.41 (d, J = 20.6 Hz, 2H), 2.87 (d, J = 64.1 Hz, 1H), 2.20 (s, 1H), 1.99 (s, 1H); HRMS (ESI) m/z calcd $C_{25}H_{27}N_6O_6$ $[M+H]^+$ 507.1992, found 507.1992.

*5.1.5 6-((1-(4-((3,4,5-Trimethoxyphenyl)amino)-5,7-dihydrofuro[3,4-d]pyrimidin-2-yl) pyrrolidin-3-yl)carbamoyl)nicotinic acid (**11**).*

Yield 22%, off-white solid. ^{1}H NMR (400 MHz, DMSO) δ: 8.95 (s, 1H), 8.59 (d, J = 14.8 Hz, 2H), 8.43 (s, 1H), 8.10 (s, 1H), 7.28 (s, 2H), 4.92 (s, 2H), 4.70 (s, 2H), 4.50 (s, 1H), 3.75 (d, J = 7.8 Hz, 7H), 3.60 (s, 5H), 3.48-3.40 (m, 1H), 2.20 (s, 1H), 2.02 (s, 1H); HRMS (ESI) m/z calcd $C_{26}H_{29}N_6O_7$ $[M+H]^+$ 537.2098, found 537.2101.

*5.1.6 6-((1-(4-((2,3-Dihydrobenzo[b][1,4]dioxin-6-yl)amino)-5,7-dihydrofuro[3,4-d]pyrimidin -2-yl)pyrrolidin-3-yl)carbamoyl)nicotinic acid (**12**).*

Yield 30%, off-white solid. ^{1}H NMR (400 MHz, DMSO) δ: 8.94 (s, 1H), 8.88 (s, 1H), 8.59 (s, 1H), 8.23 (d, J = 7.3 Hz, 1H), 7.97 (d, J = 8.1 Hz, 1H), 7.61-7.47 (m, 1H), 7.15 (d, J = 8.8 Hz, 1H), 6.77 (d, J = 8.6 Hz, 1H), 4.87 (s, 2H), 4.68 (s, 2H), 4.58 (s, 1H), 4.20 (d, J = 6.5 Hz, 4H), 3.73 (d, J = 32.8 Hz, 2H), 3.54 (s, 2H), 2.25 (s, 1H), 2.04 (s, 1H); HRMS (ESI) m/z calcd $C_{25}H_{25}N_6O_4$ $[M+H]^+$ 505.1836, found 505.1839.

5.1.7 6-((1-(4-((3,5-Dimethoxyphenyl)amino)-5,7-dihydrofuro[3,4-d]pyrimidin-2-yl)pyrrolidin

*-3-yl)carbamoyl)nicotinic acid (**13**).*

Yield 21%, off-white solid. ^{1}H NMR (400 MHz, DMSO) δ: 8.96 (s, 1H), 8.89 (s, 1H), 8.68 (s, 1H), 8.24 (d, J = 7.5 Hz, 1H), 7.98 (s, 1H), 7.19 (s, 2H), 6.12 (s, 1H), 4.90 (d, J = 25.4 Hz, 2H), 4.71 (s, 2H), 4.56 (s, 1H), 3.74 (d, J = 18.9 Hz, 8H), 3.57 (s, 2H), 2.24 (s, 1H), 2.07 (s, 1H); ^{13}C NMR (150 MHz, DMSO) δ 168.95, 166.17, 163.92, 161.08, 160.72, 154.97, 153.25, 149.55, 142.54, 139.17, 129.27, 122.48, 102.12, 98.31, 72.57, 70.96, 55.51, 49.53, 30.67; HRMS (ESI) m/z calcd $C_{25}H_{27}N_6O_4$ $[M+H]^+$ 507.1992, found 507.1997. HPLC purity: 97.8%.

*5.1.8 6-((1-(4-((4-Methoxyphenyl)amino)-5,7-dihydrofuro[3,4-d]pyrimidin-2-yl)pyrrolidin -3-yl)carbamoyl)nicotinic acid (**14**).*

Yield 28%, off-white solid. ^{1}H NMR (400 MHz, DMSO) δ: 9.00 (s, 1H), 8.62 (d, J = 32.9 Hz, 2H), 8.40 (d, J = 32.9 Hz, 1H), 8.10 (s, 1H), 7.69 (s, 2H), 6.88 (d, J = 7.7 Hz, 2H), 4.86 (s, 2H), 4.67 (s, 2H), 4.53 (s, 1H), 3.72 (s, 4H), 3.58 (s, 1H), 3.55 (s, 2H), 2.18 (s, 1H), 1.99 (s, 1H); HRMS (ESI) m/z calcd $C_{24}H_{25}N_6O_5$ $[M+H]^+$ 477.1886, found 477.1887.

*5.1.9 6-((1-(4-(p-Tolylamino)-5,7-dihydrofuro[3,4-d]pyrimidin-2-yl)pyrrolidin-3-yl)carbamoyl) nicotinic acid (**15**).*

Yield 28%, off-white solid. ^{1}H NMR (400 MHz, MeOD) δ: 8.97 (s, 1H), 8.43 (s, 1H), 8.21 (s, 1H), 7.62 (d, J = 8.0 Hz, 2H), 7.11 (d, J = 8.0 Hz, 2H), 4.91 (s, 2H), 4.76 (s, 2H), 4.67 (s, 1H), 3.90 (s, 1H), 3.74 (s, 1H), 3.63 (s, 2H), 2.34 (s, 1H), 2.29 (s, 3H), 2.15 (s, 1H); HRMS (ESI) m/z calcd $C_{24}H_{25}N_6O_4$ $[M+H]^+$ 461.1937, found 461.1940.

*5.1.10 6-((1-(4-((4-Ethylphenyl)amino)-5,7-dihydrofuro[3,4-d]pyrimidin-2-yl)pyrrolidin -3-yl)carbamoyl)nicotinic acid (**16**).* Yield 30%, off-white solid. ^{1}H NMR (400 MHz, DMSO) δ: 9.26 (s, 1H), 8.94 (s, 1H), 8.68 (s, 1H), 8.50-8.29 (m, 1H), 8.16-7.97 (m, 1H), 7.71 (s, 2H), 7.13 (d, J =

7.8 Hz, 2H), 4.89 (s, 2H), 4.68 (s, 2H), 4.59 (s, 1H), 3.79 (s, 1H), 3.57 (s, 3H), 2.55 (d, *J* = 6.1 Hz, 2H), 2.22 (s, 1H), 2.05 (s, 1H), 1.16 (dd, *J* = 8.6, 5.8 Hz, 3H); HRMS (ESI) m/z calcd $C_{25}H_{27}N_6O_4$ $[M+H]^+$ 475.2094, found 475.2094.

*5.1.11 6-((1-(4-((3,4-Dimethylphenyl)amino)-5,7-dihydrofuro[3,4-d]pyrimidin-2-yl)pyrrolidin-3-yl)carbamoyl)nicotinic acid (**17**).*

Yield 25%, off-white solid. ^{1}H NMR (400 MHz, DMSO) *δ*: 8.96 (s, 1H), 8.60 (d, *J* = 18.9 Hz, 2H), 8.39 (d, *J* = 24.9 Hz, 1H), 8.09 (d, *J* = 8.2 Hz, 1H), 7.66 (s, 1H), 7.50 (s, 1H), 7.04 (s, 1H), 4.88 (s, 2H), 4.68 (s, 2H), 4.52 (s, 1H), 3.77 (s, 1H), 3.57 (s, 3H), 2.28-2.11 (m, 7H), 1.99 (s, 1H); HRMS (ESI) m/z calcd $C_{25}H_{27}N_6O_4$ $[M+H]^+$ 475.2094, found 475.2094.

*5.1.12 6-((1-(4-(Cyclohexylamino)-5,7-dihydrofuro[3,4-d]pyrimidin-2-yl)pyrrolidin-3-yl) carbamoyl) nicotinic acid (**18**).*

Yield 29%, off-white solid. ^{1}H NMR (400 MHz, DMSO) *δ*: 9.24 (s, 1H), 8.93 (s, 1H), 8.65-8.36 (m, 1H), 8.08 (d, *J* = 10.4 Hz, 1H), 6.58 (t, *J* = 11.2 Hz, 1H), 4.76 (s, 2H), 4.59 (s, 2H), 4.56-4.44 (m, 1H), 3.86 (s, 1H), 3.74 (s, 1H), 3.55 (d, *J* = 20.0 Hz, 2H), 3.47 (d, *J* = 13.6 Hz, 1H), 2.19 (s, 1H), 1.96 (s, 1H), 1.90 (s, 3H), 1.70 (s, 3H), 1.59 (d, *J* = 11.7 Hz, 2H), 1.18-1.05 (m, 2H); HRMS (ESI) m/z calcd $C_{23}H_{29}N_6O_4$ $[M+H]^+$ 453.2250, found 453.2252.

*5.1.13 6-((1-(4-(Hexylamino)-5,7-dihydrofuro[3,4-d]pyrimidin-2-yl)pyrrolidin-3-yl)carbamoyl) nicotinic acid (**19**).*

Yield 25%, off-white solid. ^{1}H NMR (400 MHz, DMSO) *δ*: 8.91 (s, 1H), 8.86 (d, *J* = 6.4 Hz, 1H), 8.23 (d, *J* = 7.7 Hz, 1H), 7.97 (d, *J* = 8.1 Hz, 1H), 6.86 (s, 1H), 4.76 (s, 2H), 4.61 (s, 2H), 4.53 (d, *J* = 6.3 Hz, 1H), 3.76 (s, 1H), 3.62 (s, 1H), 3.50 (s, 1H), 3.47-3.42 (m, 1H), 3.32-3.25 (m, 2H), 2.18 (dd, *J* = 11.3, 7.1 Hz, 1H), 2.01 (dd, *J* = 11.2, 5.6 Hz, 1H), 1.53 (s, 2H), 1.30 (d, *J* = 26.1 Hz, 6H), 0.84 (d,

J = 6.6 Hz, 3H); HRMS (ESI) m/z calcd $C_{23}H_{31}N_6O_4$ $[M+H]^+$ 455.2407, found 455.2406.

*5.1.14 6-((1-(4-(Heptylamino)-5,7-dihydrofuro[3,4-d]pyrimidin-2-yl)pyrrolidin-3-yl)carbamoyl) nicotinic acid (**20**).*

Yield 29%, off-white solid. ^{1}H NMR (400 MHz, DMSO) δ: 9.05 (s, 1H), 8.93 (d, *J* = 6.6 Hz, 1H), 8.33 (d, *J* = 7.5 Hz, 1H), 8.06 (d, *J* = 8.1 Hz, 1H), 6.84 (s, 1H), 4.76 (s, 2H), 4.61 (s, 2H), 4.54 (d, *J* = 6.5 Hz, 1H), 3.87 (d, *J* = 23.0 Hz, 1H), 3.78 (s, 1H), 3.62 (s, 1H), 3.53 (s, 1H), 3.46 (dd, *J* = 11.5, 4.5 Hz, 2H), 2.21 (dd, *J* = 12.4, 6.5 Hz, 1H), 2.04-1.97 (m, 1H), 1.53 (s, 2H), 1.26 (d, *J* = 18.4 Hz, 8H), 0.82 (s, 3H); HRMS (ESI) m/z calcd $C_{24}H_{33}N_6O_4$ $[M+H]^+$ 469.2563, found 469.2563.

*5.1.15 6-((1-(4-(Pentylamino)-5,7-dihydrofuro[3,4-d]pyrimidin-2-yl)pyrrolidin-3-yl)carbamoyl) nicotinic acid (**21**).*

Yield 31%, off-white solid. ^{1}H NMR (400 MHz, DMSO) δ: 9.04 (s, 1H), 8.92 (d, *J* = 6.2 Hz, 1H), 8.31 (d, *J* = 8.0 Hz, 1H), 8.05 (d, *J* = 8.1 Hz, 1H), 6.83 (d, *J* = 5.2 Hz, 1H), 4.76 (s, 2H), 4.61 (s, 2H), 4.54 (d, *J* = 5.2 Hz, 1H), 3.77 (s, 1H), 3.62 (s, 1H), 3.46 (dd, *J* = 11.4, 4.5 Hz, 2H), 3.33 (s, 2H), 2.21 (dd, *J* = 13.0, 7.0 Hz, 1H), 2.05-1.99 (m, 1H), 1.54 (d, *J* = 6.5 Hz, 2H), 1.28 (d, *J* = 13.2 Hz, 4H), 0.86 (s, 3H); HRMS (ESI) m/z calcd $C_{22}H_{29}N_6O_4$ $[M+H]^+$ 441.2250, found 441.2248.

*5.1.16 6-((1-(4-((3-Methoxypropyl)amino)-5,7-dihydrofuro[3,4-d]pyrimidin-2-yl)pyrrolidin -3-yl)carbamoyl)nicotinic acid (**22**).*

Yield 20%, off-white solid. ^{1}H NMR (400 MHz, DMSO) δ: 9.06 (s, 1H), 8.95 (d, *J* = 6.4 Hz, 1H), 8.34 (d, *J* = 8.0 Hz, 1H), 8.08 (d, *J* = 8.1 Hz, 1H), 6.86 (s, 1H), 4.77 (s, 2H), 4.61 (s, 2H), 4.54 (d, *J* = 5.8 Hz, 1H), 3.79 (s, 1H), 3.62 (s, 1H), 3.53 (s, 1H), 3.49-3.45 (m, 1H), 3.36 (t, *J* = 5.9 Hz, 4H), 3.22 (s, 3H), 2.21 (dd, *J* = 12.7, 6.4 Hz, 1H), 2.05-2.00 (m, 1H), 1.79 (dd, *J* = 13.1, 6.5 Hz, 2H); HRMS (ESI) m/z calcd $C_{21}H_{27}N_6O_5$ $[M+H]^+$ 443.2043, found 443.2040.

*5.1.17 6-((1-(4-((3-Ethoxypropyl)amino)-5,7-dihydrofuro[3,4-d]pyrimidin-2-yl)pyrrolidin-3-yl) carbamoyl)nicotinic acid (**23**).* Yield 30%, off-white solid. ^{1}H NMR (400 MHz, DMSO) δ: 9.08 (s, 1H), 8.96 (d, J = 6.5 Hz, 1H), 8.36 (d, J = 8.1 Hz, 1H), 8.10 (d, J = 8.1 Hz, 1H), 6.85 (t, J = 5.3 Hz, 1H), 4.77 (s, 2H), 4.61 (s, 2H), 4.55 (d, J = 6.1 Hz, 1H), 3.80 (d, J = 16.7 Hz, 1H), 3.63 (s, 1H), 3.52 (s, 1H), 3.47 (dd, J = 11.4, 4.8 Hz, 1H), 3.39 (dd, J = 13.1, 6.5 Hz, 6H), 2.21 (dd, J = 12.7, 6.5 Hz, 1H), 2.02 (dd, J = 13.4, 7.4 Hz, 1H), 1.84-1.70 (m, 2H), 1.08 (t, J = 6.9 Hz, 3H); HRMS (ESI) m/z calcd $C_{22}H_{29}N_6O_5$ $[M+H]^+$ 457.2199, found 457.2199.

5.2 Biology

5.2.1 Kinase inhibition assays

The kinase assays were performed in the kinases buffer. Syk kinase: 50 mM HEPES pH 7.5, 0.015% Brij-35, 10 mM $MgCl_2$, 10 mM $MnCl_2$, 2 mM DTT; PDGFR-α/c-Kit kinase buffer: 50 mM HEPES pH 7.5, 0.01% Brij-35, 10 mM $MgCl_2$, 10 mM $MnCl_2$, 2 mM DTT. A 5 μL volume of tested compounds were pre-diluted for dose response in 384-well plates. A 10 μL volume of diluted enzyme solution was sequentially added and the assay plates were incubated at room temperature for 10 min, and then. And then a 10 μL volume of a mixture of peptide solution containing FAM-labeled peptide (Cat. No.112396, Lot. No. P100804-XZ112396; GL Biochem, China) and ATP (Cat. No. A7699-1G, CAS No. 987-65-5; Sigma, America) was incubated at 28 °C for 25 min. Reaction was stopped with the addition of 50 mM EDTA containing 25 μL of 100 mM HEPES, pH 7.5, 0.015% Brij-35 and 0.2% Coating Reagent #3, and the data were collected on a caliper. Half-maximal inhibition (IC_{50}) values were calculated using a non-linear curve fit with XLfit software.

5.2.2 FLSs assay

Fibroblast-liked synoviocytes (FLS; MEXN, Shanghai, China) were separated from synovial

tissues of RA patients. FLS-RA cells were maintained in high-glucose Dulbecco's Modified Eagle's Medium (DMEM; Corning, America) containing 10% fetal bovine serum (FBS; Gibco, America) at 37 ℃ in humidified environment containing 5% CO_2. FLS-RA cells from a homogeneous population were cultured for 3 generations and were used for subsequent experiments.

Antiproliferation assay was evaluated using the MTT assay performed according to the manufacturer's protocol. FLS-RA cells were seeded at a density of 2×10^4 cells/well into 96-well plates. A 1 μL volume of tested compounds of different concentrations were added into a 96-well plate (the final volume was 100 μL). Meanwhile, FLS-RA cells without inhibitors were evaluated as a control. FLS-RA cells were incubated in the medium under 5% CO_2 in an incubator maintained at 37 ℃ for 72 h, respectively. Then, a 10 μL volume of the MTT was added to each well of a 96-well incubated for additional 4 h. The absorbance was measured at 450 nm by spectrophotometer readings. All wells were incubated for 72 h at 37 ℃. Half-maximal inhibition (IC_{50}) values were calculated from 6-point dose-response curves using non-linear regression analysis.

IL-6 and MMP-3 examined by ELISA. FLS-RA cells were seeded at a density of 2×10^4 cells/well into 6-well plate, and then incubated with compounds **2**, **13**, **19** or vehicle for 30 min. After a 72 h incubation time, supernatants were collected for the determination of the IL-6 and MMP-3 levels using enzyme-linked immunoassay (ELISA) kits (Dakewe Biotech Co. Ltd., China) according to kit manufacturer's protocol.

5.2.3 mBMMCs assay

mBMMCs from the tibia and the femur of BALB/c mouse were purchased from Shanghai Slack laboratory animal co., LTD (Shanghai, China). mBMMCs were maintained at 37 ℃ in Roswell Park Memorial Institute medium (RPMI 1640 with 1% non-essential amino acid; Corning, America)

containing 10% FBS in humidified environment containing 5% CO_2. Antiproliferation assay was evaluated using MTT performed according to the manufacturer's protocol. mBMMCs were seeded at a density of 2×10^4 cells/well into 96-well plates. A 1 μL volume of tested compounds of different concentrations were added into a 96-well plate (the final volume was 100 μL). Meanwhile, mBMMCs without inhibitors were evaluated as a control. mBMMCs were incubated in the medium under 5% CO_2 in an incubator maintained at 37 °C for 48 h, respectively. Then, a 10 μL volume of the MTT was added to each well of a 96-well incubated for additional 4 h. The absorbance was measured at 450 nm by spectrophotometer readings. All wells were incubated for 48 h at 37 °C. IC_{50} values were calculated from 9-point dose-response curves using non-linear regression analysis.

TNF-α was examined by ELISA kit according to the manufacturer's instructions. mBMMCs were seeded at a density of 2×10^4 cells/well into 6-well plate, and then incubated with compounds **1**, **13**, **20** or vehicle for 30 min. After a 48 h incubation time, supernatants were collected for the determination of the TNF-α levels using ELISA kits (Dakewe Biotech Co. Ltd., China) according to kit manufacturer's protocol.

5.3 Molecular docking

The crystal structure of Syk in complex with staurosporin (a Syk inhibitor) was obtained from protein database bank (PDB ID: 1XBC[14]), which was prepared for docking using the protein preparation tool in Discovery Studio 3.0.[17] During this process, the ligands and waters were removed and hydrogens were added to the structure. Staged minimization was performed with default setting. The docking studies were carried out using GOLD 5.0.[18] Binding site was defined as whole residues within a 10 Å radius subset encompassing the staurosporin. Conformations were generated by genetic algorithm and scored using GoldScore as fitness function. The best conformation was chosen

to analyse the ligand-protein interaction. The image representing the best pose was prepared using PyMOL. Docking analysis was performed on PDGFR-α and c-Kit (PDB ID: 5GRN, 1T46, respectively)[15, 16] using a similar procedure as described above.

5.4 Statistical Analysis

Data was represented as the mean ± SD with at least three independent experiments. Comparisons between two groups were analyzed for statistical significance using Student's t test. The levels of significance were set at $P < 0.05$ (*), $P < 0.01$ (**) and $P < 0.001$ (***).

Acknowledgments

This work was supported by the National Key R&D Program of China (2017YFA0506000 to C. S.), National Natural Science Foundation of China (81725020 to C. S.), and the National Basic Research Program of China (2014CB541800 to C. S.).

A. Supplementary data

Supplementary data associated with this article can be found, in the online version, at XXXX.

References

1. Chakravarty SD, Poulikakos PI, Ivashkiv LB, et al. *Clin Immunol.* 2013;148:66-78.

2. (a) Zampeli E, Vlachoyiannopoulos PG, Tzioufas AG. *J Autoimmun.* 2015;65:1-18.

   (b) Nigrovic PA, Lee DM. *Immunol Rev.* 2007;217:19-37.

3. Paniagua RT, Sharpe O, Ho PP, et al. *J Clin Invest.* 2006;116:2633-2642.

4. Figueira MI, Cardoso HJ, Correia S, et al. *Cancer Lett.* 2017;405:10-21.

5. (a) Juurikivi A, Sandler C, Lindstedt KA, et al. *Ann Rheum Dis.* 2005;64:1126-1131.

   (b) Ando W, Hashimoto J, Nampei A, et al. *J Bone Miner Metab.* 2006;24:274-282.

6. Tebib J, Mariette X, Bourgeois P, et al. *Arthritis Res Ther.* 2009;11:R95.

7. Dubreuil P, Letard S, Ciufolini M, et al. *PLoS One.* 2009;4:e7258.

8. Zhang L, Liu W, Mao F, et al. *Arch Pharm (Weinheim).* 2015;348:463-474.

9. Braselmann S, Taylor V, Zhao H, et al. *J Pharmacol Exp Ther.* 2006;319:998-1008.

10. Cha HS, Boyle DL, Inoue T, et al. *J Pharmacol Exp Ther.* 2006;317:571-578.

11. Singh R, Masuda ES, Payan DG. *J Med Chem.* 2012;55:3614-3643.

12. Li BK, Cong Y, Yang XG, et al. *Comput Biol Med.* 2013;43:395-404.

13. (a) Padilla F, Bhagirath N, Chen S, et al. *J Med Chem.* 2013;56:1677-1692.

   (b) Lucas MC, Goldstein DM, Hermann JC, et al. *J Med Chem.* 2012;55:10414-10423.

   (c) Ellis JM, Altman MD, Bass A, et al. *J Med Chem.* 2015;58:1929-1939.

14. Atwell S, Adams JM, Badger J, et al. *J Biol Chem.* 2004;279:55827-55832.

15. Mol CD, Dougan DR, Schneider TR, et al. *J Biol Chem.* 2004;279:31655-31663.

16. Liang L, Yan XE, Yin Y, et al. *Biochem Biophys Res Commun.* 2016;477:667-672.

17. Colombano G, Travelli C, Galli U, et al. *J Med Chem.* 2010;53:616-623.

18. Jones G, Willett P, Glen RC, et al. *J Mol Biol*. 1997;267:727-748.

Graphical Abstract

Discovery of Novel Syk/PDGFR-α/c-Kit Inhibitors as Multi-targeting Drugs to Treat Rheumatoid Arthritis

Xiaokang Li,[1, †] Yahui Huang,[2, †] Junfei Chen, [2, †] Lingling Zhang,[1] Fei Mao, [1] Jin zhu,[1] Chunquan Sheng,[2,*] Jian Li[1,*]